AASCIT Journal of Chemistry
2018; 4(2): 7-17
http://www.aascit.org/journal/chemistry

Synthesis and Characterization of Electrospunned Chitosan Based Copper Nanofiber

Nurudeen Olanrewaju Sanyaolu[1, *], Sheriff Adewuyi[1], Taofik Shittu[2], Catherine Oluyemisi Eromosele[1], Nelson Torto[3]

[1]Department of Chemistry, Federal University of Agriculture Abeokuta, Abeokuta, Nigeria
[2]Department of Food Science and Technology, Federal University of Agriculture Abeokuta, Abeokuta, Nigeria
[3]Department of Chemistry, Rhodes University, Grahamstown, South Africa

Email address

nurusanya@yahoo.com (N. O. Sanyaolu)
[*]Corresponding author

Citation

Nurudeen Olanrewaju Sanyaolu, Sheriff Adewuyi, Taofik Shittu, Catherine Oluyemisi Eromosele, Nelson Torto. Synthesis and Characterization of Electrospunned Chitosan Based Copper Nanofiber. *AASCIT Journal of Chemistry.* Vol. 4, No. 2, 2018, pp. 7-17.

Received: February 7, 2018; **Accepted**: March 21, 2018; **Published**: May 16, 2018

Abstract: Fibrous materials prepared by the electrospinning process are increasingly attracting attention due to the structural advantages conveyed by the nanosized diameter of the constituent fibers. Consequently, an environmentally friendly Cu-crown chitosan nanofiber obtained from naturally available sources was developed. Chitosan derivative was synthesized via Schiff base condensation of salicylaldehyde and chitosan. The iminochitosan formed was electrospun into nanofiber mat at voltage of at 24 KV and flow rate 0.9 mLh^{-1}. The nanofiber was characterized via IR, SEM, BET, TGA and DSC and it showed a good physical stability in water and relatively high heat capacity. Kinetic study shows that the sorption of copper using chitosan nanofiber follows a pseudo-first order equation. The description of the isotherm can best be done using the Langmuir isotherm model. The maximum sorption capacity and sorption affinity constant were calculated as 500.00 mg g^{-1} and 0.34704 Lmg^{-1}. Desorption capacity 92% was obtained using $(NH_4)SO_4$ as regenerant. The copper-nanofiber mix has a high potency for use in industries as a result of its good water stability, favourable heat capacity, high adsorption capacity and good recyclability.

Keywords: Electrospinning, Nanofiber, Iminochitosan, Pretreatment

1. Introduction

The quest of bringing a new research impetus for catalyst development at the interface between homogeneous and heterogeneous catalysis has led to the introduction of catalyst support. A typical example is chitosan, an optically active biopolymeric ligand that is characterized by a strong affinity for transition metals [1-3]. The biopolymer can be used as a support for the preparation of heterogeneous catalysts in the form of colloids, flakes, gel beads and more importantly fibers [4-8, 2]. Nanofibers are characterized by large surface area which makes them to be an excellent matrix for catalyst support, enabling metal dispersion as small particles and inhibiting the sintering of the active catalyst material.

There are a few different methods to produce fibers *vis-a-vis* phase separation [9], drawing [10], template synthesis [11-14] and self assembly [15-19]. However, the unique synthetic method of electrospinning, has received much attention lately. With electrospinning, the structure, chemical and mechanical stability, functionality, and other properties of the mats can be modified to match end applications [20, 21]. Also, the fibers are nano only in diameter and form a mat like three-dimensional structure making separation from solution very simple and as such ideal candidates as catalyst supports [22].

Although, Copper (II) metal ion has been complexed with chitosan for various purposes [5, 8, 23-25], there are few examples in which coordination based metal-immobilization with nanofibrous chitosan strategy has been adopted. Worthy of mentioning is the work of Bradshaw et al. (2011) [22] which successfully catalyzed a Heck cross-coupling reaction between iodobenzene with n-butyl acrylate using Pd(II) complexed chitosan nanofiber. Cu (II) ion can form a variety of complexes with coordination numbers from 4–6 [26]. Due to their flexibility, facility of preparation and capability of

stabilizing unusual oxidation states and successful performance in mimicking particular geometries around metal centers, they have very interesting spectroscopic properties and varied catalytic activities [27]. It is important, from our point of view that Cu(II) complexes of nanofiber based chitosan polymeric ligand will not only serve as good candidate but as well as biocompatible, inexpensive catalyst for oxidation or hydrolysis within a wide range of pH.

In order to obtain an electrospinnable chitosan solution, an iminochitosan derivative synthesized via Schiff base condensation of salicylaldehyde and chitosan was adopted [28]. The excellently formed nanofiber was then carefully coordinated to Cu(II) ions to form the solid state chelate. The spectroscopic characterization, thermogravimetry as well as the morphological state of this new catalyst material is herein reported.

2. Methods

Analytical grade (AR) chemicals with highest purity were used. Scanning Electron Microscopy machine used was Vegan Tescan (TS5136ML) operating at an accelerated voltage of 20 KV after gold soutler coating for the morphology of the electrospunn imminochitosan. The quantitative analysis of Cu(II) was done using Atomic Absorption Spectrophotometer. A magnetic stirrer with hotplate was used for the batch adsorption experiments. A thermogravimetric analyser model TA-2960 was employed to determine thermogravimetric curves using Ca. 10 mg samples of the imminochitosan materials in a dynamic atmosphere, under a dry nitrogen flux, with heating from room temperature to 800°C at a heating rate of 10°C/min^{-1}. Differential Scanning Calorimeter model DSC (TAQ10) was used. The temperature and heat flow were calibrated using standard materials (indium and zinc) at cooling and heating rates of 10°C/min. Samples with a typical mass of 3–10 mg were encapsulated in sealed aluminum pans).

2.1. Synthesis of Iminochitosan

Imminochitosan was prepared by a Schiff base reaction between chitosan (100 g) and salicylaldehyde (130 ml) in 1.5 liter of water at room temperature for 6 hours. The modified chitosan was filtered and washed with distilled water several times. Methanol extraction was done in soxhlet for 6 hours. The product was dried at room temperature for 24 hours to obtain the final iminochitosan [29].

2.2. Preparation of Iminochitosan Solution for Electrospinning

A flask containing the iminochitosan and triflouroacetic acid (TFA) was placed in acetone/dry ice bath and frozen. It was then thawed in a water bath at ambient temperature. The iminochitosan dissolved in the TFA very quickly as a result of the sudden freezing and thawing. The solution was left overnight. After that the solution was ready to be electrospun. The electrospinning solution was electrospunned at the following conditions; 5-24 KV, 0.1-1.0 mlh^{-1}, 5-20 cm, 1.2 mm needle, 44.9%, 17.3°C [29].

2.3. Post Neutralization of Iminochitosan

Neutralization of the as-spun iminochitosan nanofiber mats was carried out in a 1 molL^{-1} K_2CO_3 aqueous solution for 3 h at 25°C. The nanofiber mat was taken out from the aqueous solution after neutralization, washed repeatedly with deionized water until a pH 7 was achieved, and dried first at an ambient temperature for 24 h in the hood and then at 60°C under vacuum for 24 h [30].

2.4. Stability in Water and Water Retention of Chitosan Nanofiber

The degree of stability of the nanofiber mat in terms of weight loss in the aqueous solution was examined at pH 7 and an ambient temperature.

The degree of stability (S) of the nanofiber (rectangular shape of 3cm by 1cm in size) was expressed by the following equation:

$$S(\%) = \frac{W_1 - W_2}{W_1} \times 100 \quad (1)$$

Where, W_1 and W_2 are weights of the dried nanofibers before and after the experiment respectively [30]. Nanofiber was weighed in an electronic balance with 0.1 mg resolution and incubated in distilled water at room temperature for 2 hours 40 minutes and it was re-weighed immediately after removing them from water.

The percentage water uptake of the electrospun membranes was calculated using the following equation:

$$Water\ uptake\ (\%) = \frac{M_1 - M_0}{M_0} \times 100 \quad (2)$$

where, M_o and M_1 were the masses of the membranes before and after the incubation of the samples in water, respectively [30, 31].

2.5. Cu impregnation of the Post-Neutralised Iminochitosan Nanofiber

The nanofiber was pre-treated by first heating to 30°C for 10 minutes after which it was heated in vacuum under nitrogen atmosphere for 6 hours. The method of impregnation was adopted for the imobilization of the Cu(II) on the electrospunned nanofiber. The dried sample (0.05 g) of the post-neutralised iminochitosan was placed in glass beaker and a stock solution of $CuSO_4$ (1g/L) was added untill all the nanofiber was completely immersed [32]. Then, the mixture was filtered and the nanofiber was rinsed several times with the copper stock solution and then once with water. Finally, the chitosan samples were dried at room temperature until all moisture was removed and constant weight achieved.

2.6. Adsorption Kinetic Study

A stock solution (1000 mg/L) of Cu(II) ions was prepared from analytical-reagent grade Cu metal (BDH). Adsorption kinetic study was conducted in 250 ml Erlenmeyer flask containing 0.010 g (M) of adsorbent (chiotosan nanofiber) and 100 mL of copper catalyst source solution prepared by dillution of the stock solution to 100 mg/L. The mixture was

equilibrated using a magnetic stirrer at a speed of 150 rpm at 30 ± 1°C. At appropriate time intervals of 10, 20, 30, 40, 50, 60, 80, 100 and 360 min, aliquot samples were withdrawn, filtrated and analysed for residual Cu concentration (*Ce)* by flame atomic absorption spectrophotometry. The amount adsorbed (q) was calculated from the following formula:

$$q = \frac{(C_o - C_e)V}{M} \quad (3)$$

Where, "V" is the volume of the suspension [33].

2.7. Adsorption Isotherm Study

Adsorption isotherm experiments of copper on chitosan nanofiber were conducted by firstly preparing a series of 100 ml copper solutions with concentrations 100, 200, 300, 400 and 500 mg/L and 0.01 $molL^{-1}$ Na_2SO_4 solution was added to each and the pH were adjusted to 6.0 using 0.10 M HNO_3 or 0.10 M NaOH. The adsorbent 0.01 g chitosan nanofiber was added into the mixtures and were equilibrated at a speed of 150 rpm for 40 minutes at 30 ± 1°C. At appropriate time intervals of 10, 20, 30, 40, 60 and 360 minutes, aliquot samples were withdrawn, filtrated and analysed for residual copper concentration by flame atomic absorption spectrophotometry.

2.8. Batch Desorption Experiments

The desorption experiments were conducted by placing 18.8, 37.5 and 56.3 mg of copper-crown nanofiber (containing 0.5, 1.0 and 1.5 integra values of the maximum adsorption capacity respectively) each in contact with the regenerating solution of 25 ml of 1 M $(NH_4)_2SO_4$ separately at room temperature using an agitation speed of 100 rpm for 2 hours. The mixtures were filtered and the amount of desorbed metallic ions in the filtrate was determined using the flame atomic absorption spectrophotometry as stated before. The percentage of desorption (DP) were calculated using the equation below [23, 34]

$$DP\ (\%) = \frac{C_a - C_d}{C_a} \times 100 \quad (4)$$

Where C_a and C_d are the concentration of metal ions desorbed and adsorbed (mgL^{-1}). The desorption process were carried out in triplicates.

3. Results

Synthesis of Iminochitosan

SEM

A fine fiber was formed when iminochitosan was freez dried in TFA and electrospunn (Figure 1). The iminochitosan was further characterised using FT-IR, TG and DSC. Figure 2 shows the SEM image of the synthesized iminochitosan that was electropsunn in TFA at optimum conditions.

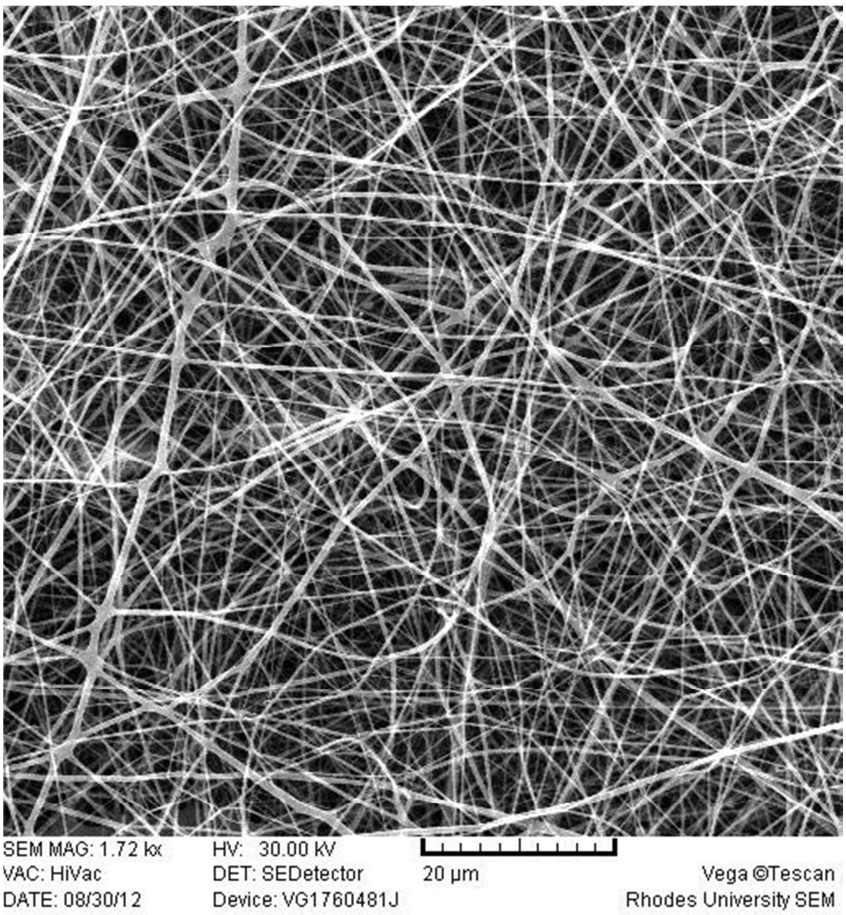

Figure 1. *Scanning electron micrographs of electrospun chitosan: 4-6% chitosan with 100 g of 130 ml salicyaldehyde with 1.5L of Deionized water in TFA, 5-24 KV, 1.2 mm, 5-20 cm, 0.1-1.0 m/h, 44.9% 17.3°C.*

Thermal Properties

Figure 2 shows the analysis of iminochitosan by TGA in the temperature range 20 to 550°C nitrogen and air atmospheres. The iminochitosan shows high degree of stablity to change in temperature; the onset temperature of degradation was high. It can be found that the nanofiber show little change in weight loss over a wide range of temperature.

In Figure 3, a differential scanning calorimetry (DSC) curve for the proposed catalyst support is shown, the curve shows distinct deviations from the usual steplike changes in heat flow. The curve is characterised by the following peaks; a broad endothermic peak in the range of 100 – 150°C, and exothermic peaks at around 390, 490 and 520°C.

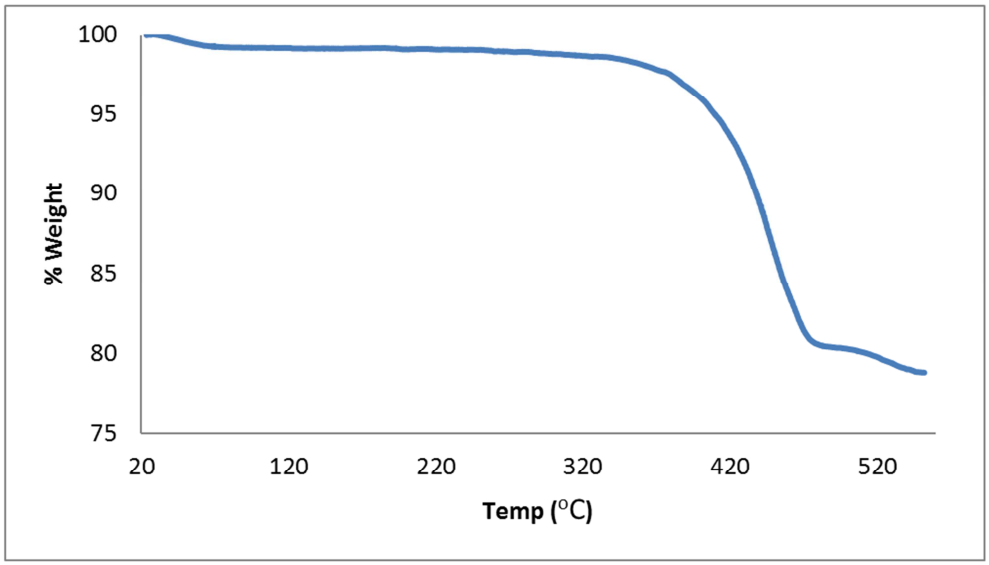

Figure 2. *TGA curve of iminochitosan nanofiber under nitrogen atmosphere.*

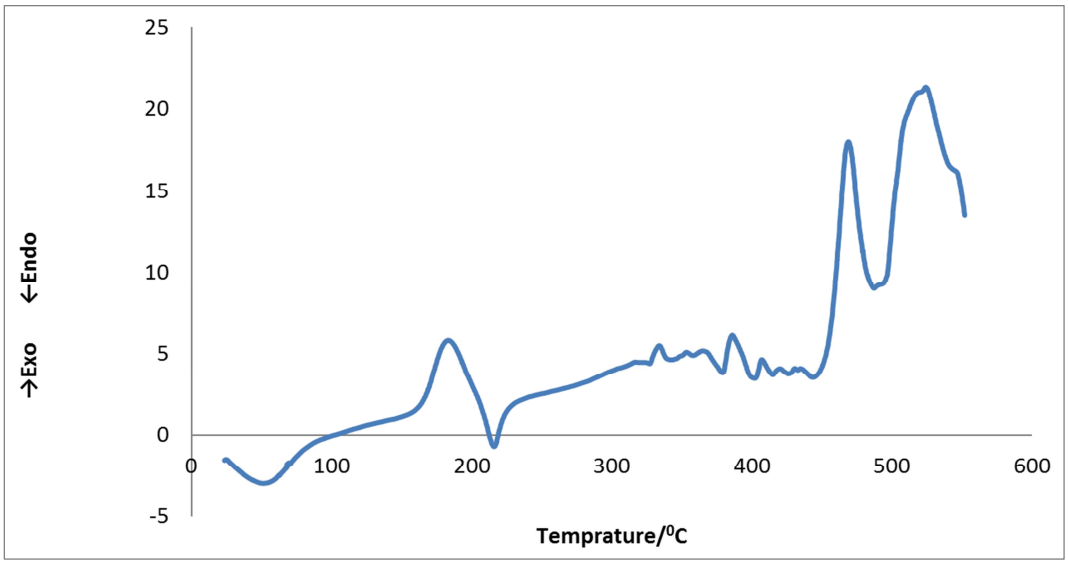

Figure 3. *DSC of the iminochitosan nanofiber.*

Post-neutralisation

Chitosan was soluble in triflouroacetic acid as a result of the formation of the salts ($NH_3^+CF_3COO^-$) of ammonium (-NH_3^+) and trifluoroacetate (CF_3COO^-) ions in the nanofibers. However, the presence of the salts will lead to and unfavourable interaction of the ammonium ions on the chitosan nanofibers with the positively charged metal ion. The introduction of the neutralising agent (K_2CO_3) will lead to the re-introduction of amine group which will improve the adsorption sites for positively charged metal ion and also improve the stability of the nanofiber in aqeous solution.

Figure 4 shows the scanning electron micrographs of the post-neutralised electrospun iminochitosan.

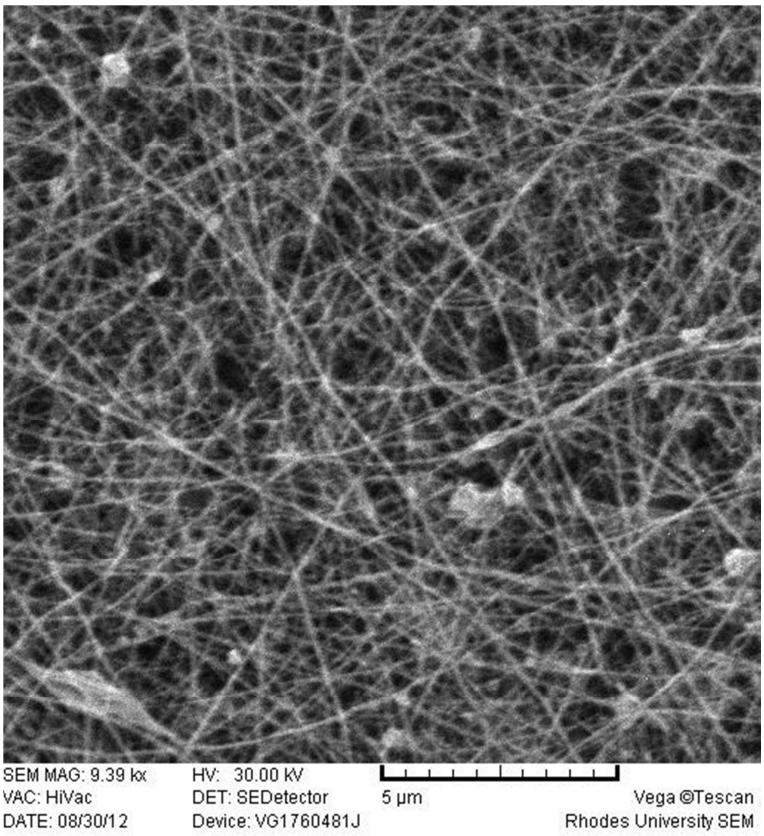

Figure 4. *Scanning electron micrographs of post-neutralised electrospun iminochitosan.*

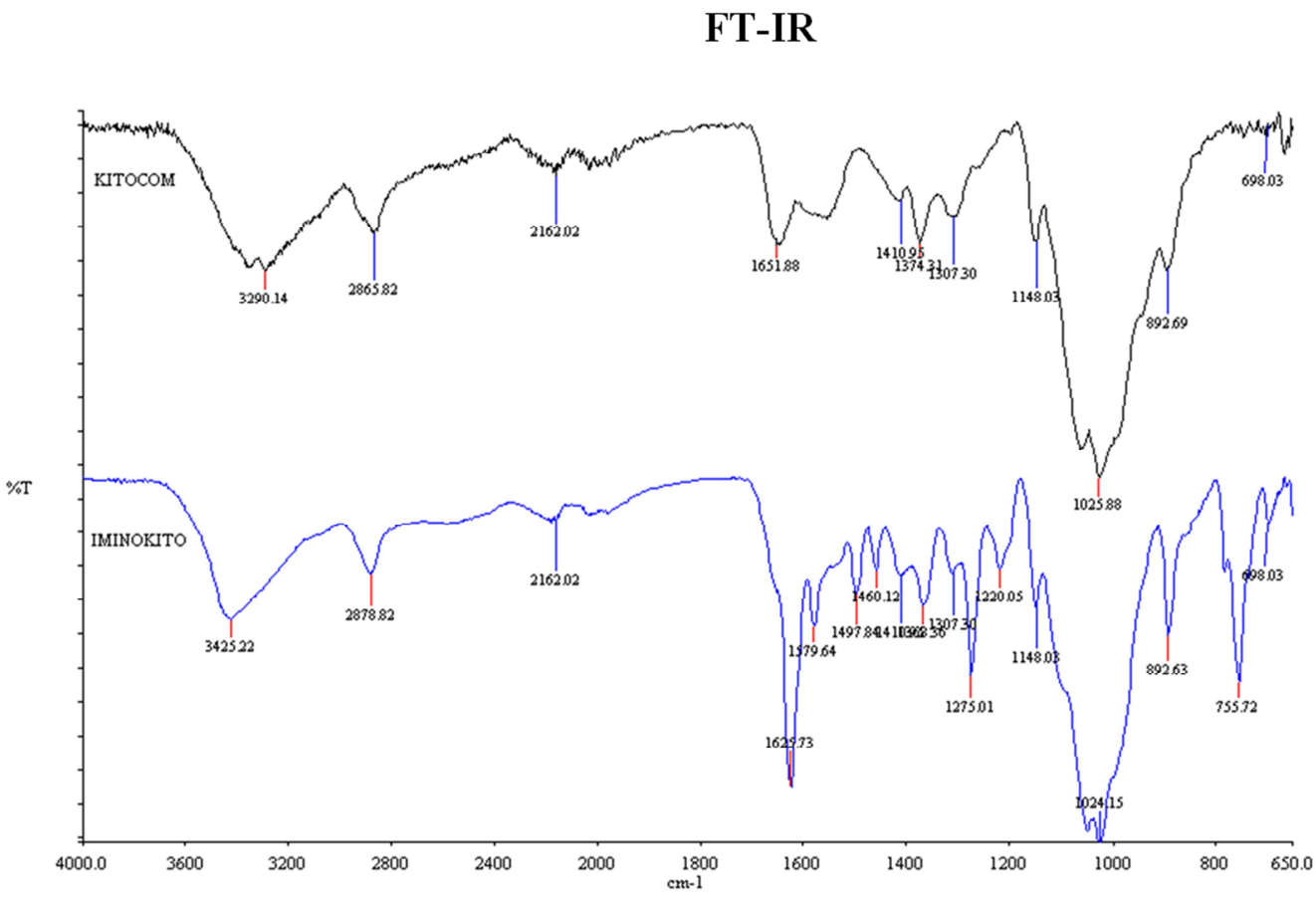

Figure 5. *FT-IR spectra of as-spun imminochitosan nanofibrous membranes in comparison with that of post-neutralised iminochitosan nanofiber.*

The fibers were found to be in the range 70 - 200 nm. The FTIR data of iminochitosan reveals an increase in the percentage of C and H, whereas the percentage of N decreased in Figure 5, the absorption peak of the chitosan NH_2 (at 3339 and 3420 cm^{-1}) disappeared after formation of iminochitosan (-N=CH). This indicates that all the amino groups were masked.

Stability in water and Water Retention of Post-neutralised Iminochitosan Nanofiber

The loss in the weight of the iminochitosan nanofibrous membrane also increased very rapidly during the first three days of submersion, but, after fifteen days, no significant change was observed (Figure 6). In analogy to the weight loss, the degree of swelling for the chitosan derivative membrane increased initially with submersion period, but became unchanged after a certain submersion period (Figure 7).

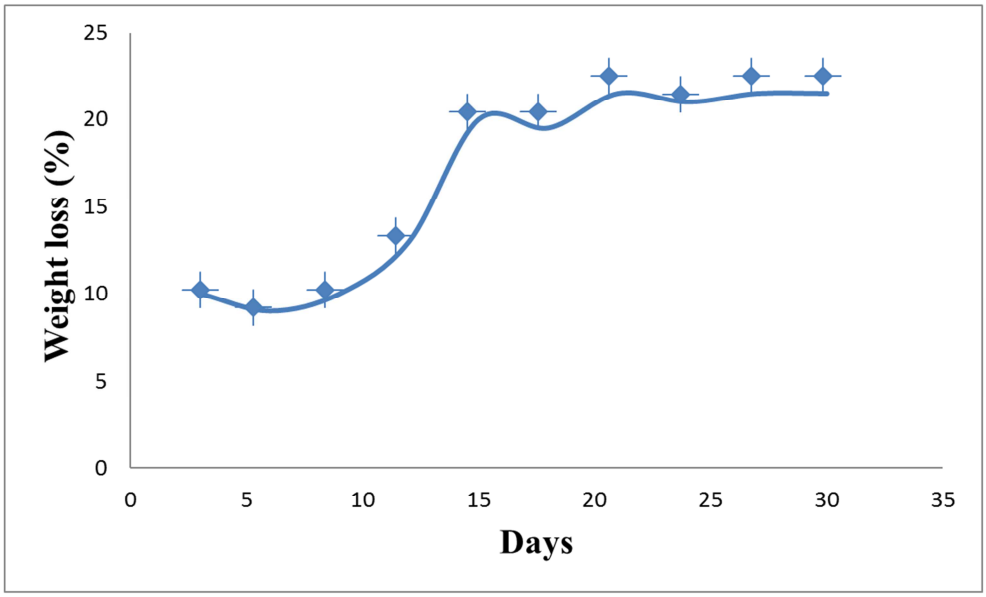

Figure 6. *Weight loss of the post-neutralised iminochitosan adsorbent.*

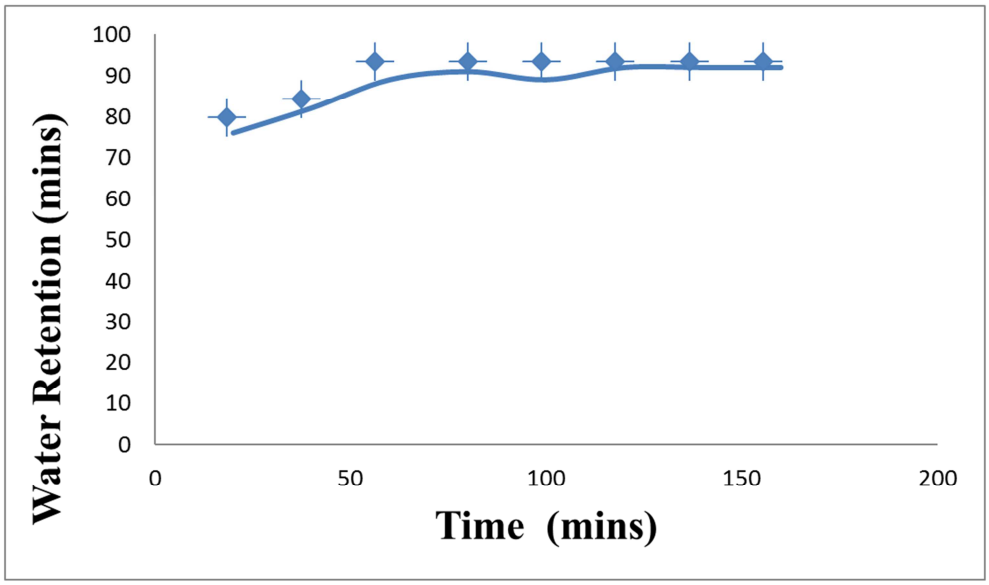

Figure 7. *Water Retention property of the post-neutralised iminochitosan adsorbent.*

FT-IR Cu impregnation of the post-neutralised iminochitosan nanofiber

Figures 8 and 9 shows the far infra-red spectroscopy of the post-neutralised iminochitosan nanofiber adsorbent and post-neutralised iminochitosan-copper mix. Cu(II) bonding causes a noticeable change in the shape of the broad absorption line at 150–100 cm^{-1} typical of different types of (–OH, –NH) vibrations in polymers. Complexation of Cu(II) ions by the post-neutralised iminochitosan matrix results in substantial redistribution of vibration frequencies in the above-mentioned region, with a shift to lower wavenumbers [5].

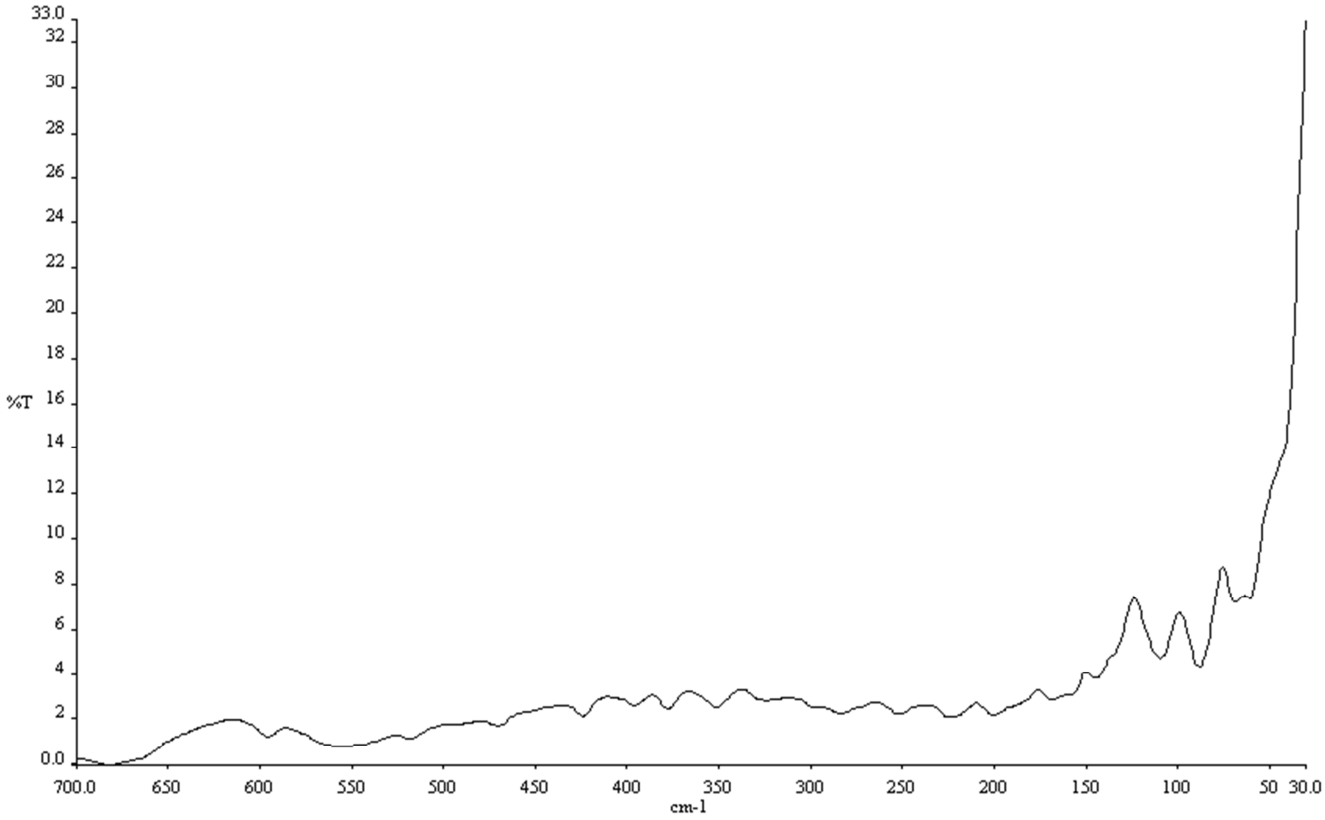

Figure 8. *Far IR of post-neutralised Iminochitosan.*

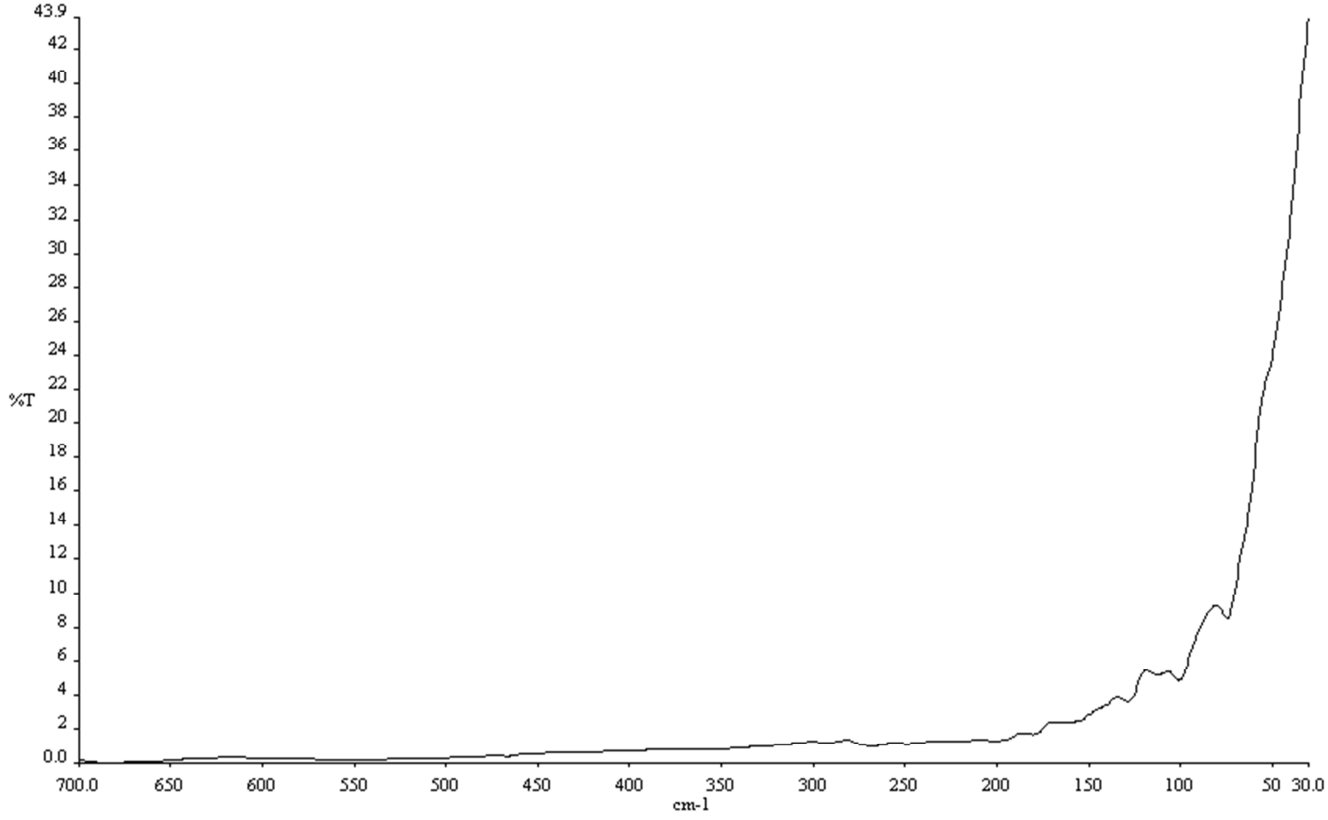

Figure 9. *Far IR of Cu impregnated iminochitosan.*

Adsorption Kinetic Study

The adsorption of Cu(II) ion onto the chitosan nanofiber mat in a 100 ppm copper solution as a function of time until 360 mins at a pH of 6.0 is shown in Figure 10. The

adsorption amount of copper metal increased sharply from 5 mins to 30 mins and then leveled off after 40 mins at 33.9027 mg g^{-1} for Cu(II). It can be deduced from the shape of the curve that the equilibrium was reached at 30 mins that is, the binding of metal ions to the chelating sites on the adsorbent increased sharply up to 30 mins and was homogeneously saturated after 40 mins [38].

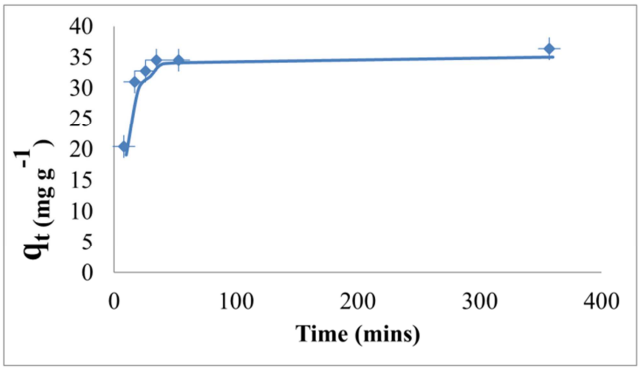

Figure 10. *Adsorption of the Cu(II) ion onto chitosan nanofiber in a 100 ppm synthetic solutions as a function of time.*

Adsorption isotherm Study

Figure 11 is a linearized plot of C_e/q_e versus C_e and it shows that the Langmuir equation best fits for Cu(II) adsorption on the chitosan nanofiber under the concentration range studied (correlation coefficient, R>0.99).

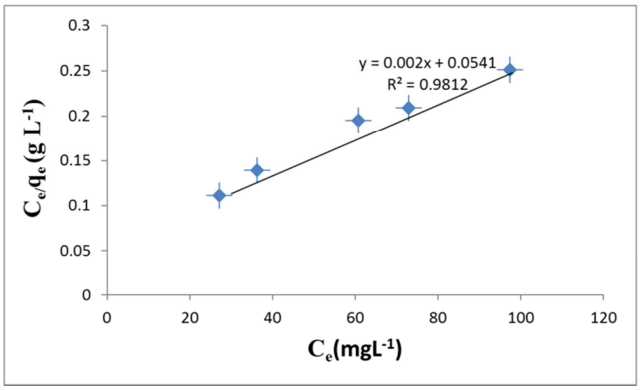

Figure 11. *Adsorption isotherms of copper.*

The adsorption increased rapidly as the initial concentration increased and then the slope of the increased decreased as the further concentration increased (graph not shown). The high surface area coupled with the inter and intrafibrous pores of the nanofiber which is devoid of gases and the available binding sites (such as amine, primary and secondary hydroxyl groups) might be responsible for the observed increased in the adsorption rate [39, 40].

Desorption Study

Figure 12 shows the result of the desorption experiment carried on different weights of the copper loaded chitosan nanofiber. The percentage desorption 60, 90 and 88% were obtained for the different weights 18.8, 37.5 and 56.3 respectively.

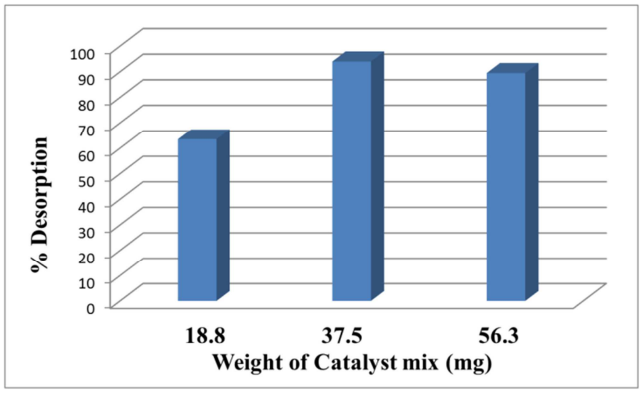

Figure 12. *Desorption studies of copper from different weight of the copper-crown nanofiber with $(NH_4)SO_4$ as regenerants (Temperature 30°C: pH 1). Values were represented as Mean of 3 Readings.*

4. Discussion

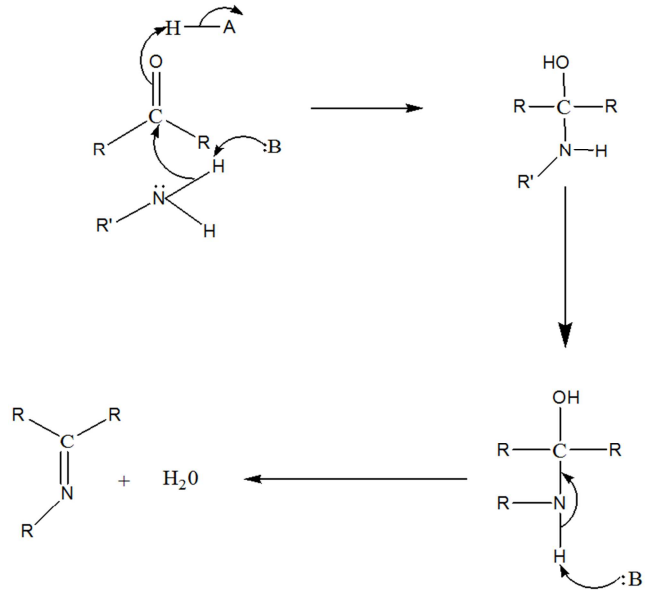

Figure 13. *Synthetic scheme for iminochitosan.*

The synthetic route for iminochitosan is shown in Figure 13 where the carbon atom of salicylaldehyde was subjected to nucleophilic attack by the primary amine of the chitosan. The Schiff base condensation on chitosan has overcome its rigid crystalline structure, improved the viscousity and solubility thereby leading to the formation of uniform iminochitosan fiber. This is in a good agreement with the submissions of Marine [41] and Nada [42].

The thermal property of the iminochitosan (Figure 2) revealed that there was insignificant weight loss between the temperature range 20-420°C; the temperature at which 5% weight loss occurred was 420°C. It can also be observed that there were two decomposition stages; one well-defined stage within the temperature range 350–500°C and another above 500°C these values are relatively higher when compared to the likely temperature when being put into use [43]. The weight loss around 100°C and 320°C can be attributed to adsorbed water molecule and the decomposition of

polysaccharide respectively [35].

The first endothermic peak is related to the evaporation of water molecules in the nanofiber but the area and position of the endothermic peaks was large and at a higher temperature. This suggests that the nanofibers has a high water holding capacity and strong interaction with water molecules. However, the exothermic peak which supposed to be observed clearly at 274°C due to the decomposition of amino (GlcN) has been signigicantly reduced meaning that it has been masked. The exothermic peaks around 390, 490 and 520°C can be attributed to the decomposition of the N-acetyl (GlcNAc) residues [36; 44], due to the thermal decomposition of imine (C=N) and benzene ring (C_6H_6) residues, respectively (Figure 3).

The Schiff base condensation has affected the morphology, size and diameter of the post neutralised. This account for the differences observed in the micographs [39; 40; 45]. The presence of salts can also affects some other properties like cellular affinity, degradation, structural and pore size [46; 47].

Scanning electron microscopy (SEM) of the postneutralised iminochitosan revealed a thicker fiber which can be attributed to the increase in the polymer concentration.

The disappearance of the imine bond at the vibrational frequency of 1630 to 1640 cm^{-1} in the post-neutralised iminochitosan confirms the efficacy of the neutralisation process while the absorption bands of amine and aldehyde groups at 1560 and 1665cm^{-1} affirms that the chitosan structure has not been disrupted.

A two step pattern was observed in the physical integrity test in terms of weight loss of the post-neutralised iminochitosan in water for over thirty days (Figure 6); 80% of the weight lost was observed in within the first fifteenth days and the remaining fifteen days, there were no significant weight loss. The water content of nanofiber is very important; it gives a reflection of the ionization of functional groups in the electrospun fibers for the adsorption reaction. It points to the fact that as an addendum to metal chelation on the outer surface as a route for adsorption, metal ions also diffuse onto the pores of the nanofiber [37].

Characterisation of the Cu impregnated nanofiber (Figure 8) further supports the metal chelation property of the post-neutralised nanofiber.

Adsorption Isotherms

Table 1 shows different adsorption capacities of copper (II) ion onto different adsorbents. The values ranges from 0.17 to 2.94 (mmol/g) with the highest values obtained in chitosan fiber (this work). Furthermore, chitosan nanofiber which was not pretreated was found to have maximum adsorption capacity of 2.85 mmol/g while the pretreated one has 2.94 mmol/g. The differences in the value can be accounted for as a result of the pretreatment which activated the pores by removing the gases therein.

Table 1. *Comparison of the adsorption capacities of Cu^{2+} onto different adsorbents.*

Adsorbents	qm (mmol/g)
Activated nylon-based membrane	0.17[48]
Clinoptilolite	0.40[49]
Polymer modified pine bark	0.70[50]
Thiourea-modified chitosan microspheres	1.04[51]
Cu(II) ion imprinted composite adsorbent	1.12[52]
Poly(acrylamide)/attapulgite	1.64 -1.81[53]
St-g-PAA	2.80[54]
St-g-PAA/5% SH	2.83[54]
Chitosan nanofiber	2.85[31]
Pretreated Chitosan nanofiber	2.94

Table 2 shows the parameters indicating the isotherm shape [55] while table 3 shows the values of R_L calculated for different initial Cu (II) on chitosan nanofiber mat. By comparism, the parameter quantifying the relative affinity of the Cu (II) ion for the surface adsorption values (R_L) obtained shows that favourable adsorption of Cu (II) on chitosan nanofiber took place, therefore, chitosan nanofiber is a good adsorber. The values of the Langmuir binding energy, *b* in the system is high (greater than 0.1) and it is related to the free energy of sorption of different solutes. A high value of *b* implies the metals are adsorbed at high energy surfaces with low dissociation constants while lower *b* values indicate the adsorption of metals at low energy surfaces with high dissociation constants [56].

Table 2. *Effect of separation factor on isotherm shape [55].*

R_L Value	Type of isotherm
$R_L > 1$	Unfavourable
$R_L = 1$	Linear
$0 < R_L < 1$	Favourable
$R_L = 0$	Irreversible

The R_L values calculated for the different initial Cu (II) ion on chitosan nanofiber are given in Table 3

Table 3. *R_L values based on the Langmuir equation.*

Cu (II) Initial Concentrations (mg/L)	R_L values
100	0.026
200	0.013
300	0.009
400	0.007
500	0.005

Desorption study

This study gives an insight into the nature of the adsorption process and how to recover the Cu(II) ion from the nanofiber. This study will also serve to be a means of reducing cost of procurement of chitosan nanofiber as it can be regenerated and reuse again.

5. Conclusions

Iminochitosan was successfully synthesized and electrospunn at optimum conditions. The fibers formed are characterised by fine diameter. The metal adsorption was successfully impregnated on the fiber and it was aided by the pretreament given to the nanofiber. The equilibrium time for the adsorption was 30 mins and the equilibrium data fits well with the Langmuir isotherm model maximum adsorption

capacity and adsorption affinity constant of 500.00 mg g^{-1} and 0.34704 Lm g^{-1} respectively. The isothermal shape indicate a favourable adsorption and the desorption study shows that the nanofiber can be regenerated and reused which makes the process to be economical.

Acknowledgements

The author wish to acknowledge the following;
a. Staffs and students of Chemistry Department, Rhodes University, Grahams Town, South Africa
b. Staffs and students of Chemistry Department, Federal University of Agriculture, Alabata, Abeokuta, Nigeria.

References

[1] Adewuyi S, Kareem KT, Atayese AO, Amolegbe SA, Akinremi CA (2011) Chitosan–cobalt(II) and nickel(II) chelates as antibacterial agents. Internat. Journ of Bio Macromol *48*: 301-303.

[2] Guibal E (2005) Heterogeneous catalysis on chitosan-based materials: A review. Prog Polym Sci 30: 71-109. doi: 10.1016/j.progpolymsci.2004.12.001.

[3] Baba Y, Hirakawa H, Yoshizuka K, Inoue K, Kawano Y (1994) Adsorption Equilibria of Silver(I) and Copper(II) Ions on N-(2-Hydroxylbenzyl)chitosan Derivative. Analytical Sciences 10: 601.

[4] Kramareva NV, Stakheev AY, Tkachenko OP, Klementiev KV, Grünert W, Elena D. Finashina ED, Kustov LM (2004) Heterogenized palladium chitosan complexes as potential catalysts in oxidation reactions: study of the structure. Journal of Molecular Catalysis A: Chemical 209: 97-106. doi: 10.1016/j.molcata.2003.08.004.

[5] Kucherov AV, Kramareva NV, Finashina ED, Koklin AE, Kustov LM (2003) Heterogenized redox catalysts on the basis of the chitosan matrix 1. Copper complexes. Journal of Molecular Catalysis A: Chemical 198: 377-389. doi: 10.1016/S1381-1169(03)00002-5.

[6] Ohkawa K, Minato K, Kumagai G, Hayashi S, Yamamoto H (2006) Chitosan Nanofiber. Biomacromolecules 7: 3291-3294.

[7] El-hefian EA, Nasef MM, Yahaya AH (2011) Chitosan Physical Forms: - Short Review. Australian Journal of Basic and Applied Sciences 5 (5): 670-677.

[8] Antony R, David ST, Karuppasamy K, Saravanan K, Thanikaikarasan S, Balakumar S (2012) Structural, surface, thermal and catalytic properties of chitosan supported Cu(ii) mixed ligand complex materials. journal of surface engineered materials and advanced technology 2: 284-291 Argun ME, Dursun S, Karatas M (2009) Removal of Cd(II), Pb(II), Cu(II) and Ni(II) from water using modified pine bark. Desalination 249: 519-527.

[9] Ma PX, Zhang R (1999) Synthetic nano-scale fibrous extracellular matrix. J Biomed Mat Res. Part A 46 (1): 60-72.

[10] Ondarcuhu T, Joachim C (1998) Drawing a single nanofibre over hundreds of microns. Europhys Lett 42 (2): 215-20.

[11] Feng L, Li S, Li H, Zhai J, Song Y, Jiang L (2002) Super-Hydrophobic Surface of Aligned Polyacrylonitrile Nanofibers. Angew Chem Int Ed 41 (7): 1221-3.

[12] Martin CR (1996) Membrane-based synthesis of nanomaterials. Chem Mater 8: 1739-46.

[13] Li H, Ke Y, Hu Y (2006) Polymer nanofibers prepared by template melt extrusion. J Appl Polym Sci 99 (3): 1018-1023.

[14] Ikegame M, Tajima K, Aida T (2003) Template synthesis of polypyrrole nanofibers insulated within one-dimensional silicate channels: Hexagonal versus lamellar for recombination of polarons into bipolarons. Angew Chem Int Edit 42 (19): 2154-2157.

[15] Liu GJ, Ding JF, Qiao LJ, Guo A, Dymov BP, Gleeson JT, et al. (1999) Polystyrene-block-poly (2-cinnamoylethyl methacrylate) nanofibers-Preparation, characterization, and liquid crystalline properties. Chem-A European J 5: 2740-2749.

[16] Whitesides GM, Grzybowski B (2002) Self-assembly at all scales. Science 295: 2418-21.

[17] Yang Z, Xu B (2007) Supramolecular hydrogels based on biofunctional nanofibers of self-assembled small molecules. J Mater Chem 17 (23): 2385-2393.

[18] Feng X, Yang G, Xu Q, et al. (2006) Self-assembly of polyaniline/Au composites: From nanotubes to nanofibers. Macromol Rapid Comm 27 (1): 31-36.

[19] Hong Y, Legge R L, Zhang S (2003) Effect of amino acid sequence and pH on nanofiber formation of self-assembling peptides EAK16-II and EAK16-IV. Biomacromolecules 4 (5): 1433-1442.

[20] Mart´ınez-Camacho AP, Cortez-Rocha MO, Castillo-Ortega MO, Burgos-Hern´andez A, Ezquerra-Brauera JM, Plascencia-Jatomea M (2011) Antimicrobial activity of chitosan nanofibers obtained by electrospinning. Polym Int 60: 1663-1669. DOI 10.1002/pi.3174.

[21] Sun K, Li ZH (2011) Preparations, properties and applications of chitosan based nanofibers fabricated by electrospinning. eXPRESS Polymer Letters 5 (4): 342-361. DOI: 10.3144/expresspolymlett.2011.34.

[22] Bradshaw M, Zou J, Byrne L, Swaminathan-Iyer K, Stewart S. G, Raston, C. L (2011) Pd(II) conjugated chitosan nanofibre mats for application in Heck cross-coupling reactions. Chem Comm 47: 12292-12294.

[23] Futalan CM, Tsai W, Lin S, Dalida ML, Wan M (2012) Copper, nickel and lead adsorption from aqueous solution using chitosan-immobilized on bentonite in a ternary system. Sustain Environ Res 22 (6): 345-355.

[24] Boey HT, Tan WL, AbuBakar NHH, Bakar MA, Ismail J (2007) formation and morphology of colloidal chitosan-stabilized copper sulfides. Journal of Physical Science 18 (1): 87-101.

[25] Chiessi E, Gaio P, Mariano V, Baribio P (1992) Copper complex immobilized to Chitosan. Journal of Inorganic Biochemistry 46: 109-118.

[26] Hathawy BJ (1987) Comprehensive Coordination Chemistry. Pergamon, Oxford 5: 533.

[27] Fenton DE (1999) Metallobiosites and their synthetic analogues—a belief in synergism 1997–1998 Tilden Lecture. Chem Soc Rev 28: 159-168.

[28] El-Tahlawy K, Abdelhaleem E, Hudson SM, Hebeish A (2007) Acylation of Iminochitosan: Its Effect on Blending with Cellulose Acetate. Journal of Applied Polymer Science 104: 727-734. DOI 10.1002/app.24136.

[29] Nawalakhe RG (2009) Improving Healing Performance of Wound Dressing: Electrospinning of Chitosan-based, Cellulose-based Fibers and their Blends. Dissertation, North Carolina State University 90-98.

[30] Haider S, Park SY (2009) Preparation of the electrospun chitosan nanofibers and their applications to the adsorption of Cu(II) and Pb(II) ions from an aqueous solution. J Membr Sci 328: 90-96.

[31] Zhang YZ, Venugopal J, Huang ZM, Lim CT, Ramakrishna S (2006) Crosslinking of the electrospun gelatin nanofibers. Polymer 47: 2911-2917.

[32] Ye Z, Alsyouri H, Zhu S, Lin YS (2003) Catalyst impregnation and ethylene polymerization with mesoporous particle supported nickel-diamine catalyst. Polymer 44: 969-980.

[33] Shashidhar T, Philip L, Bhallamudi M (2006) Bench-scale column experiments to study the containment of Cr(VI) in confined aquifers by bio-transformation. Journal of Hazardous Materials 131: 200-209.

[34] Benavente M, Arévalo M, Martínez J (2006) Speciation and Removal of Arsenic in Column Packed with Chitosan. Water Practice & Technology 1 (4): 4-8. doi: 10.2166/WPT.2006.0089. ISSN 1751-231X.

[35] Sik NM, Park WH, Daewoo IHM, Hudson, SM (2010) Effect of the degree of deacetylation on the thermal decomposition of chitin and chitosan nanofibers. Carbohydrate Polymers 80: 291-295.

[36] Sangsanoh P, Supaphol P (2006) Stability improvement of electrospun chitosan nanofibrous membranes in neutral or weak basic aqueous solutions. Biomacromolecules 7: 2710-2714.

[37] Bokgi S, Yeom BY, Song SH, Lee C. S, Hwang TS (2008) Antibacterial Electrospun Chitosan/Poly(vinyl alcohol) Nanofibers Containing Silver Nitrate and Titanium Dioxide. Journal of Applied Polymer Science Wiley Periodicals, Inc. 111: 2892-2899.

[38] Saeed K, Haider S, Oh TJ, Park SY (2008) Preparation of amidoxime-modified polyacrylonitrile (PAN-oxime) nanofibers and their applications to metal ions Adsorption. J Membr Sci 322: 400-405.

[39] Maria P, Raffaela B, Mario G, Antonella P (1993) Sorption mechanism of trace amount of divalent metal ions on a chelating resin containing iminodiacetate groups. Anal Chem 65: 2522-2527.

[40] Rangel-Mendez JR., Monroy-Zepeda R, Leyva-Ramos E, Dˇıaz-Flores PE, Shirai K (2009) Chitosan selectivity for removing cadmium (II), Copper (II), and lead (II) from aqueous phase: pH and organic matter effect. J Hazard Mater 162: 503-511.

[41] Luminita M, Iuliana S, Mihai M, Valentina D, Bogdan CS, Mihail B (2013) Antifungal vanillin–imino-chitosan biodynameric films. Journal of Materials Chemistry B12: 20-35.

[42] Ahmed AN, Roshan J, Namdev BS, Matthew DH, Hassan MA, Rajaram KN, Sangamesh GK (2014) A smart methodology to fabricate electrospun chitosan nanofiber matrices for regenerative engineering applications. Polym. Adv. Technol. 25: 507-515.

[43] Nam YS, Won HP, Daewoo I, Samuel MH (2010) Effect of the Degree of Deacetylation on the Thermal Decomposition of Chitin and Chitosan Nanofibers. Carbohydrate Polymers 80: 291-295.

[44] Ingrid C, Roberto N, Francesco T, Maria GF, Flavia F, Silvia T, Giuliana M (2015) Advanced physico-chemical characterization of chitosan by means of TGA coupled on-line with FTIR and GCMS: Thermal degradation and water adsorption capacity. Polymer Degradation and Stability 1: 112.

[45] Saad BQ, Muhammad SZ, Shariq N, Zohaib K, Altaf HS, Shehriar H, Ihtesham UR (2018). Internationa l Journal of Molecular Sciences. Electrospinning of Chitosan-Based Solutions for Tissue Engineering and Regenerative Medicine. Int. J. Mol. Sci. 19: 407.

[46] Qasim SB, Rehman IU (2018) Application of Nanomaterials in Dentistry. In Micro and Nanomanufacturing Volume II; Springer: Berlin, Germany. 2: 319-336.

[47] Bhardwaj N, Kundu SC (2010) Electrospinning: A fascinating fiber fabrication technique. Biotechnol. Adv. 28: 325-347.

[48] He, ZY, Nie HL, White CB, Zhu LM, Zhou YT, Zheng Y (2008) Removal of Cu^{2+} from aqueous solution by adsorption onto a novel activated nylon-based membrane. Bioresource Technol 99: 7954-7958.

[49] Sprynskyy M, Buszewski B, Terzyk, AP, Namiésnik J (2006) Study of the selectionm mechanism of heavy metal (Pb^{2+}, Cu^{2+}, Ni^{2+}, and Cd^{2+}) adsorption on clinoptilolite. J Colloid Interf Sci 304: 21-28.

[50] Argun ME, Dursun S, Karatas M (2009). Removal Of Cd(II), Pb(II), Cu(II) and Ni(II) from Water using Modified Pine Bark. *Desalination* 249: 519-527.

[51] Zhou L, Wang Y, Liu Z, Huang Q (2009) Characteristics of equilibrium, kinetics studies for adsorption of Hg(II), Cu(II), and Ni(II) ions by thiourea-modified magnetic chitosan microspheres J Hazard Mater 161: 995-1002.

[52] Ren Y, Zhang M, Zhao D (2008) Synthesis and properties of magnetic Cu(II) ion imprinted composite adsorbent for selective removal of copper. Desalination 228: 135-149.

[53] Xhen H, Wang, A (2009) Adsorption characteristics of Cu(II) from aqueous solution onto poly(acrylamide)/attapulgite composite. J Hazard Mater 165: 223-231.

[54] Yian Z, Shuibo H, Aiqin W (2010) Adsorption behavior of Cu^{2+} from aqueous solutions onto starch-g-poly (acrylic acid)/sodium humate hydrogels. Desalination 263: 170-175.

[55] Ngah WS, Endud CS, Mayanar R (2002) Removal of copper (II) ions from aqueous solution onto chitosan and cross-linked chitosan beads. Reactive & Functional Polymers 50: 181-190.

[56] Oh S, Kwak MY, Shin WS (2009) Competitive sorption of lead and cadmium onto sediments. J Chem Eng 152: 376-388.